In an earlier work[17] it was recognized that back-diffusion was a major problem. It was easily avoided by use of a long path length (approximately 3 m) between the reaction vessel and the pumping system itself. Unfortunately back-diffusion was considered to be an obvious gas kinetics problem, and it was not specifically pointed out in the published article. This and similar problems have arisen in low-pressure studies of this type and have frequently been overlooked. In the experiment reported here back-diffusion is avoided by use of an effusion orifice where a high pressure ratio is maintained across the hole (Figure 1).

In several studies the recombination of oxygen atoms on a surface or back-diffusion itself has reduced the steady-state O-atom concentration at a given point in the system. Titration results for example are then in error since the reaction used ($NO_2 + O \rightarrow NO + O_2$) is very fast and results in titrating all the oxygen atoms flowing into a reaction chamber. The number in the steady state, however, is normally reduced by consumption on the walls of the vessel and by back-diffusion of recombined oxygen.

The results presented here are compatible with the simple two-body reaction mechanism propounded in earlier papers.[17,20] This does not eliminate the possibility of two operating reaction mechanisms, the second being the three-body reaction with an intermediate excited state. Other low-pressure experiments reported in the literature which support the latter mechanism frequently fail to account for such problems as back-diffusion. The work at Bonn[21] does support our earlier conclusions.

Acknowledgment. The authors wish to acknowledge the aid of Roger W. Waldron with many of the experimental details. This work was supported by the National Aeronautics and Space Administration through Grant NGR 33-018-086.

(20) D. Appelbaum, P. Harteck, and R. Reeves, *Photochem. Photobiol.*, 1, 1003 (1965).

(21) (a) K. H. Becker, A. Elzer, W. Groth, P. Harteck, and D. Kley, "Simulation von physikalisch-chemischen Vörgangen in der höheren Atmosphäre," Part 1, SHA/1, Institute fur Physicalische Chemie der Universität Bonn, Dec 1968; (b) K. H. Becker, A. Elzer, W. Groth, and D. Kley, *ibid.*, Part 2, SHA/2.

Molecular Modulation Kinetic Spectrometry. ClOO and ClO_2 Radicals in the Photolysis of Chlorine in Oxygen

Harold S. Johnston, Earl D. Morris, Jr., and Jack Van den Bogaerde

Contribution from the Department of Chemistry and the Inorganic Materials Research Division, Lawrence Radiation Laboratory, University of California, Berkeley, California 94720.
Received August 22, 1969

Abstract: By means of the new molecular modulation method, the gas-phase absorption spectra of the peroxyl radical ClOO has been observed between 2300 and 2600 Å (ultraviolet) and between 1430 and 1460 cm^{-1} (infrared). This radical was produced by the photolysis of Cl_2 in the presence of O_2. The ultraviolet spectrum of the ClO radical was also observed, but its infrared spectrum could not be obtained by this method. By direct observation of these two intermediates, a detailed kinetic study was carried out, in which radical half-lives were inferred from observed phase shifts between the square-wave photolyzing light and the radical concentration. To enhance the weak signals from the low concentration radicals, the data were put in digital form and long-term averaging was carried out. The mechanism built up by previous workers was modified slightly to give a ten-step mechanism, which is in excellent agreement with observations. By combining other rate measurements, thermodynamic data, and the present results, seven out of the ten elementary rate constants were evaluated, and a product-and-ratio of the other three was evaluated as one term. The absolute cross section for absorption of infrared and ultraviolet radiation by ClOO was determined.

Porter and coworkers[1-3] postulated the ClOO peroxy radical as a short-lived precursor to the ClO radical which they detected in the flash photolysis of chlorine–oxygen mixtures. On the basis of the very small temperature coefficient of ClO formation, Porter and Wright[2,3] concluded that the only plausible reaction by which ClO could be formed is

$$Cl_2 + h\nu \xrightarrow{a} 2Cl$$
$$Cl + M + O_2 \underset{c}{\overset{b}{\rightleftharpoons}} ClOO + M \qquad (1)$$
$$ClOO + Cl \xrightarrow{d} 2ClO$$

They observed that the decomposition of ClO to Cl_2 and O_2 occurs relatively slowly, has a negligible activation energy, and is second-order with respect to ClO, and the rate is independent of Cl_2, O_2, and total gas pressures

(1) G. Porter, *Discussions Faraday Soc.*, 9, 60 (1950).
(2) G. Porter and F. J. Wright, *Z. Elektrochem.*, 56, 782 (1952).
(3) G. Porter and F. J. Wright, *Discussions Faraday Soc.*, 14, 23 (1953).

ranging from 55 to 610 Torr. They ruled out a direct decomposition of the type

$$2ClO \longrightarrow Cl_2 + O_2 \qquad (2)$$

because of the high activation energy usually associated with such a reaction and suggested that the overall reaction probably proceeds *via* the dimer Cl_2O_2 (eq 3).

$$\begin{aligned} 2ClO &\rightleftharpoons Cl_2O_2 \\ Cl_2O_2 &\longrightarrow Cl_2 + O_2 \end{aligned} \qquad (3)$$

Porter and Wright omitted a chaperon molecule in this mechanism since they observed independence of the overall rate on total pressure.

The work of later investigators substantiated the second-order recombination of ClO radicals; however, the reported rate constants show a wide disagreement. In these studies ClO was produced by the flash photolysis of OClO,[4] ClOCl,[5] and Cl_2–O_3 mixtures.[6] The kinetics of ClO has also been studied in flow discharge systems[7] reacting Cl or O atoms with OClO. Durie and Ramsay[8] carried out a detailed rotational–vibrational analysis of the ultraviolet spectrum of ClO produced in flash photolysis of Cl_2–O_2 mixtures. They showed the dissociation energy of the ground state is 63.31 ± 0.03 kcal/mole. Thus, for ground-state $Cl(^2P_{3/2})$ atoms, the reaction $2Cl + O_2 \rightarrow 2ClO$ is exothermic by 8.66 ± 0.10 kcal/mole. Burns and Norrish[9] reinvestigated the mechanism of ClO formation in the flash photolysis of Cl_2–O_2 mixtures. They were able to confirm that ClO is produced predominantly in a reaction of ground-state Cl atoms with O_2, thus supporting the reaction scheme of Porter and Wright which requires the existence of the ClOO radical.

Benson and Buss[10] proposed that the bimolecular disappearance of ClO takes place *via* the ClOO peroxy radical

$$\begin{aligned} 2ClO &\xrightarrow{e} ClOO + Cl \\ ClOO + M &\underset{b}{\overset{c}{\rightleftharpoons}} Cl + O_2 + M \\ Cl + ClOO &\xrightarrow{f} Cl_2 + O_2 \end{aligned} \qquad (4)$$

They suggest that since the rapid reaction d is evidently responsible for ClO formation in photolysis of Cl_2–O_2 mixtures, the nearly thermoneutral reverse reaction e might be expected to be the rate-determining step for ClO removal. These same authors showed further that the observed rate law for the Cl_2-catalyzed decomposition of N_2O cannot be explained by a nonchain reaction, but is consistent with a Cl atom chain in which Cl atoms are regenerated by the decomposition of ClO. In further support of the existence of the ClOO radical, Benson and Buss suggested that the participation of this species seemed to be the only way of accounting for the long chain lengths observed in the photolytic decompositions of OClO and ClOCl, and the chain character of the explosions which both of these are known to undergo. These investigators also made use of the experimental observations of earlier workers to estimate the thermodynamic properties of the peroxy ClOO radical.

In a recent investigation, Clyne and Coxon[11] obtained convincing evidence that at low pressures, near 1 Torr, ClO radicals are removed predominantly by the free-radical mechanism proposed by Benson and Buss (eq 4). This work was carried out in a discharge–flow system, in which a pure stream of ClO radicals was generated by the rapid reaction of Cl atoms with OClO. They were able to make a distinction between the two mechanisms for ClO recombination by the introduction to the ClO system of a substrate capable of reaction with atomic Cl. Clyne and Coxon determined the activation energy of the ClO recombination reaction to be 2.5 ± 0.3 kcal/mole, whereas Porter and Wright had found a zero activation energy for this reaction. Furthermore, they noted that their measured second-order rate constant at 298°K was significantly lower than that obtained by other workers at the considerably higher pressures utilized in flash photolysis. They reconciled these discrepancies by postulating that at higher pressures an unstable intermediate such as Cl_2O_2 is formed by an equilibrated, overall third-order reaction involving the participation of a chaperon molecule. However, they did not directly observe or demonstrate an inert gas effect in this reaction.

Several inconclusive attempts to observe the ClOO peroxy radical directly were made before its eventual unambiguous detection. Benson and Anderson[12] found that Cl_2–O_2 mixtures, when exposed to near-ultraviolet light and then trapped at liquid N_2 temperatures, yield a solid Cl_2 matrix which on subsequent warming liberates small quantities of O_2 in excess of that trapped mechanically in the absence of light. Rochkind and Pimentel,[13] studying the *in situ* photolysis of matrix-isolated ClOCl at 20°K, observed a pair of weak infrared bands at 1428–1438 cm^{-1} which they attributed to a photolysis product of OClO impurity. They tentatively assigned the doublet to ClOO because of its similarity to that of the FOO analog, in which case the observed band would be due to the slightly perturbed stretch of an O_2 molecule to which a Cl atom was weakly bound. Utilizing electron spin resonance, Symons and coworkers[14] have obtained spectra that may be ClOO in several low-temperature, irradiated, solid-state systems.

Arkell and Schwager[15] were able to report the direct spectroscopic detection and identification of the ClOO peroxy radical in a recent investigation. They produced the elusive species most readily by photolysis of OClO in an argon matrix, as well as by photolysis of Cl_2 in normal and isotopically substituted oxygen matrices at 4°K. The ClOO radical in argon was found to have fundamental infrared absorptions at 1441, 407, and 373 cm^{-1}. Isotopic work with $Cl_2 + O_2$ (50% $^{18}O_2$) gave observed absorptions which supported the

(4) F. J. Lipscomb, R. G. W. Norrish, and B. A. Thrush, *Proc. Roy. Soc., Ser. A*, 233, 455 (1956).
(5) F. H. C. Edgecombe, R. G. W. Norrish, and B. A. Thrush, *ibid.*, 243, 24 (1957).
(6) W. D. McGrath and R. G. W. Norrish, *ibid.*, 254, 317 (1960).
(7) M. A. A. Clyne and J. A. Coxon, *Trans. Faraday Soc.*, 62, 1175 (1966).
(8) R. A. Durie and D. A. Ramsay, *Can. J. Phys.*, 36, 35 (1958).
(9) G. Burns and R. G. W. Norrish, *Proc. Roy. Soc., Ser. A*, 271, 289 (1963).
(10) S. W. Benson and J. H. Buss, *J. Chem. Phys.*, 27, 1382 (1957).
(11) M. A. A. Clyne and J. A. Coxon, *Proc. Roy. Soc., Ser. A*, 303, 207 (1968).
(12) S. W. Benson and K. H. Anderson, *J. Chem. Phys.*, 31, 1082 (1959).
(13) M. M. Rochkind and G. C. Pimentel, *ibid.*, 46, 4481 (1967).
(14) R. S. Eachus, P. R. Edwards, S. Subramanian, and M. C. R. Symons, *Chem. Commun.*, 1036 (1967); *J. Chem. Soc., A*, 1704 (1968).
(15) A. Arkell and I. Schwager, *J. Am. Chem. Soc.*, 89, 5999 (1967).

assignment of the 1441-cm^{-1} band to the O–O stretching vibration. Final confirmation that the observed infrared spectrum belongs to the ClOO radical resulted from the use of ^{18}O-substituted OClO, which gave isotopic infrared absorptions which were in excellent agreement with calculated values obtained from the normal coordinate analysis. The observation of a quartet in both the O–O and Cl–O stretching regions demonstrated the nonequivalence of the two O atoms and substantiated the Cl–O–O structure.

The chlorine–oxygen system has been reinvestigated in this laboratory using the new kinetic and spectroscopic method of molecular modulation.[16,17] An absorption spectrum of another intermediate in addition to ClO has been detected in the ultraviolet. This has been assigned to the ClOO radical proposed earlier.[16b] In the present work further experiments using both ultraviolet[18] and infrared[19] spectra have confirmed the participation of ClOO in the formation of ClO. Since we are able to follow the concentration of ClOO spectroscopically, new kinetic information is obtained.

Experimental Method

General Description. In kinetic studies of complex reactions it is highly desirable to observe the free-radical intermediates by spectroscopic means. This permits one to confirm the participation of a particular radical species in the reaction mechanism without disturbing the system. Further, absorption spectra of these intermediate species yield valuable structural and thermodynamic information. Finally, in the case of complex mechanisms involving three or more intermediates, it is impossible to deduce a unique mechanism solely by analysis of all reactants and products.[2c] The indeterminacy lies in the fact that there are more elementary reactions than independent observables. Additional information is obtained by direct spectroscopic observation of the intermediate species.

One method of studying the spectra of free radicals and the processes by which they are destroyed is to generate a high initial concentration with a short, intense pulse of light. One then monitors the concentration decay by spectroscopic means. Flash photolysis coupled with flash spectroscopy is an example of this approach. The reaction mechanism can be quite different from that at high light intensities. It is the situation involving relatively low concentrations of free radicals in which we are interested and for which our experimental method is designed.

A limit to the precision with which an absorption intensity measurement can be made is set by the number of photons available during the time of measurement. An obvious means of improving the precision in an experiment limited by a weak spectroscopic source is to average the information from a number of replicate measurements. The molecular modulation method consists of switching a photolytic source on and off (square-wave) in order to produce an oscillating concentration of free radicals. If spectroscopic light is passed through this system, its intensity at wavelengths characteristic of the radicals formed will also oscillate. Detection of this chemically modulated light and integration by electrical means then provides a free radical absorption signal. In this way, very low-level absorption intensities from a large number of flashing cycles can be averaged to give a more precise measurement.

Ultraviolet fluorescent lamps generate fluxes in the range of 10^{14}–10^{16} photons/(cm^2 sec). This intensity produces free-radical concentrations of the order of 10^{10}–10^{13} particles/cm^3. Given a typical infrared cross section and a path length of 80 m, an optical absorption of 10^{-4} can be expected. In the system where ultraviolet light is used to observe the intermediates, the cross section for light absorption is typically more than an order of magnitude larger than in the infrared. Since the ultraviolet cell has a path length of only 4 m, the expected modulation is about the same in each system.

From the intensity of photolyzing light in our systems and the range of rate constants, radical lifetimes should be between 10 and 0.025 sec. Consequently the photolytic light must be switched at frequencies from 0.1 to 40 Hz in order to obtain a reaction period that is comparable to the lifetime of the radical being investigated. The resulting signal falls in the low-frequency region where electronic noise that varies as reciprocal frequency ($1/F$) is predominant and presents a serious experimental problem. The problem of detecting small ac signals buried in noise has been attacked by utilizing the technique of phase-sensitive lock-in detection. Radical lifetimes can be inferred by determination of the phase shift of the modulation with respect to the photolytic excitation. The problem of $1/F$ noise is avoided by allowing the concentration oscillations to modulate a chopped 400-Hz carrier beam (ir or uv) transferring the chemical information to side bands centered at 400 Hz. Thus initial amplification of the low level signal can be done at frequencies sufficiently high that $1/F$ noise is no longer important. The use of amplitude modulation also makes it possible to separate chemical signal from noise or scattered light generated by the photolysis source.

Both kinetic and spectroscopic information regarding the free radical of interest is available from this experimental technique. Spectroscopic information requires a determination of absorption intensity *vs.* wavelength. This is carried out by scanning slowly through a given spectral region, flashing the photolytic lamps at one fixed frequency. The spectroscopic beam will be modulated in regions characteristic of an absorber whose concentration is oscillating. A spectrum is scanned slowly enough that background spectra due to the light source or stable molecules are filtered out electronically.

Kinetic measurements to ascertain the lifetime of a particular radical are carried out after its absorption bands have been located and identified. The phase shifts of the modulated signal relative to the ultraviolet light are determined at various flashing frequencies. In the phase shift method an excitation cycle consists of equal periods of light and dark. Spectroscopic measurements are made during the intervals of radical buildup as well as decay. The calculations that are involved in evaluating radical lifetime and reaction order from the measured phase have been described.[16c]

The effect of intermittent ultraviolet illumination upon a photolabile chemical system is to cause a periodic variation in the concentration of the species attacked directly by light. Ensuing reactions bring about concentration oscillations of other reactants, intermediates, and products. Consequently, when scanning through a particular spectral region, the appearance of a modulation signal may be due to a reactant or product, as well as an intermediate. This method of spectroscopic detection is sensitive only to changes in concentration so that modulated signals from reactants, intermediates, and products are all of the same order of magnitude, although their individual concentrations may differ by a factor of 10^6. As described before,[16a] the phase shift itself is diagnostic as to whether the modulated signal is reactant, intermediate, or product.

Infrared Apparatus.[19] A diagram of the experimental apparatus and instrumentation is presented in Figure 1. The reaction cell is a cylindrical steel vessel, *ca.* 2.2 m in length, 0.40 m i.d., and 270 l. volume. The inner surface was coated with a low vapor pressure, inert varnish. Conventional gas handling and purification equipment is used to regulate the flow rate and composition of gases into the cell. Gold-plated mirrors are mounted 2.0 m apart at the ends of the cell, and by multiple reflections an optical path of 72 m is obtained. The ultraviolet photolysis lamp (GE 65-W, "black-light" fluorescent lamp, F40 BL/5, useful length 1.2 m) is mounted longitudinally inside the cell in front of curved Alzak aluminum (high uv reflectivity) reflectors. The monochromator is a Beckman IR-7 prism-grating instrument. The 400-Hz mechanical chopper is driven by a synchronous motor locked to a highly stable tuning fork oscillator. The detector is a mercury-doped germanium photoconductor (Santa Barbara Research Center) cooled with liquid helium. The purpose of the carrier demodulator is to separate

(16) (a) H. S. Johnston, G. E. McGraw, T. T. Paukert, L. W. Richards, and J. Van den Bogaerde, *Proc. Nat. Acad. Sci. U. S.*, 57, 1146 (1967); (b) E. D. Morris, Jr., and H. S. Johnston, *J. Am. Chem. Soc.*, 90, 1918 (1968); (c) G. E. McGraw and H. S. Johnston, *J. Chem. Kinetics*, 1, 89 (1969).

(17) E. D. Morris, Jr., and H. S. Johnston, *Rev. Sci. Instrum.*, 39, 620 (1968).

(18) E. D. Morris, Jr., Ph.D. Dissertation, University of California, Berkeley, 1969.

(19) J. M. Van den Bogaerde, Ph.D. Dissertation, University of California, Berkeley, 1969; Lawrence Radiation Laboratory Report, UCRL-18682.

(20) H. S. Johnston and F. Cramarossa, *Advan. Photochem.*, 4, 1 (1965).

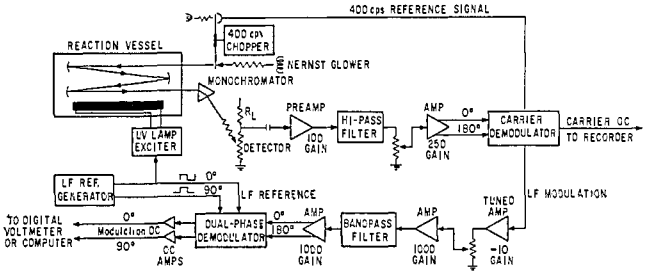

Figure 1. Schematic diagram of experimental system with infrared detection of intermediates.

the modulated side bands at 400 ± F from the 400-Hz carrier signal. The dual-phase demodulator resolves the in-phase and 90° out-of-phase components of the modulated signal, permitting a determination of both phase and amplitude. The low-frequency reference generator provides two square waves exactly 90° apart in phase. One of these signals triggers the photolytic lamp. Both are needed in the low-frequency dual-phase demodulator. The tuned amplifier serves as an active filter while all other amplifiers are wide band. The preamplifier is battery powered. All other amplifiers have well-regulated power supplies.

Ultraviolet Apparatus.[18] The basic system is analogous to that used in the infrared, although several new features were developed, especially the digital lock-in system. These new features are described elsewhere.[16b,17] The reaction cell is a quartz cylinder 1.8 m long and 15 cm i.d. with a single mirror at one end. Two photolysis lamps were mounted outside the cell and backed by Alzak aluminum reflectors. The spectrometric light over the region 2000–3500 Å is provided by a deuterium lamp (Bausch and Lomb DE-50A) powered by a well-stabilized power supply. A tuning fork (American Time Products) operating at 400 Hz chops the spectrometric beam at the cell entrance. The fork also provides a 400-Hz reference used in the detection system. A McPherson (Model 218, 0.3 m) monochromator equipped with a 2400-line/mm grating follows the reaction cell. An EMI photomultiplier (9526B) is mounted at the exit slit of the monochromator.

The output of the photomultiplier and the 400-Hz reference from the tuning fork are fed into a 400-Hz lock-in amplifier which separates the magnitude of the spectrometric light and the low-frequency modulation signal. A crystal oscillator is scaled down to control the photolysis lamps and to provide reference signals to compare with the modulated signal. The signal and references are sent to a digital lock-in[17] where long-time averaging is obtained by means of reversible counters. The magnitude of the in-phase and 90° lag components is digitalized and punched into paper tape. This tape is later fed into a computer which calculates phase shift and modulation amplitude at each wavelength of the spectrometric light.

Intensity of Photolyzing Radiation. The intensity of the photolyzing ultraviolet light was found by following the rate of decay of NO_2. This method requires exact values of the absorption coefficient of NO_2 as a function of wavelength (2700–4400 Å), quantum yield over the same range of wavelength, the spectral distribution of the photolyzing fluorescent lamp, and the full set of rate constants for the elementary reactions in this system (involving NO_2, NO, O, O_2, O_3, NO_3, and N_2O_5). To calculate the rate of production of Cl, it was necessary to combine the above data with the absorption coefficient of Cl_2 over the same range of wavelengths. Full details are given in the thesis of Van den Bogaerde.[19]

In the infrared apparatus the average ultraviolet light intensity was 8.5×10^{15} photons/(cm² sec), and the cross section for light absorption by chlorine weighted by the spectral distribution of the lamps used was 0.935×10^{-19} cm². Thus the rate of destruction of chlorine molecules is

$$\mathrm{d} \ln [Cl_2]/\mathrm{d}t = aI_0 = 0.80 \times 10^{-3} \text{ sec}^{-1} \quad (5)$$

In the ultraviolet apparatus the photolyzing intensity is larger because two lamps are used and the cell has a small diameter.

$$I_0 = 4.2 \times 10^{16} \text{ photons/(cm}^2 \text{ sec)} \quad (6)$$

$$aI_0 = 3.92 \times 10^{-3} \text{ sec}^{-1} \quad (7)$$

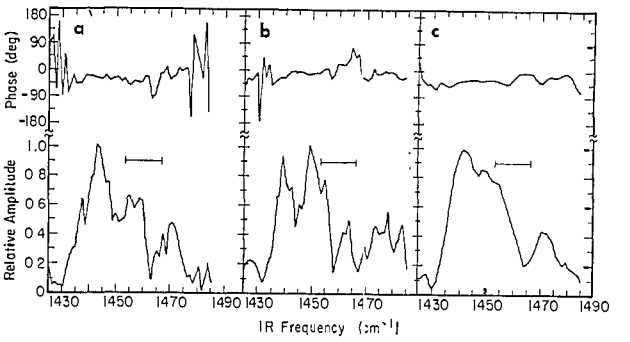

Figure 2. ClOO infrared molecular modulation spectrum observed with 4 Torr of Cl_2, 189 Torr of O_2, 567 Torr of He, 2-Hz square-wave ultraviolet photolysis: (a) 40 scans; (b) duplicate, another set of 40 scans; (c) smoothed cumulative measurements, 80 scans (a and b). |—| indicates spectral slit width.

Results

Infrared Spectroscopic Measurements. Exploratory scans were carried out over a fairly wide spectral region. The region from 800 to 200 cm⁻¹ was scanned using a 100-sec time constant. A reaction mixture of 4 Torr of Cl_2 and 756 Torr of O_2 flashed at 1 Hz. From these preliminary measurements, a single chemically modulated absorption band was detected at 1410–1490 cm⁻¹. This absorption exhibited the phase shift expected[16a] for a primary intermediate species, and on this basis, as well as its position,[15] the band was tentatively attributed to the ClOO radical.

The region of 1400–1520 cm⁻¹ was subjected to a more intensive investigation by scanning repeatedly at a speed of 8 cm⁻¹/min. A spectrometer slit width of 6 mm was used which corresponds to a spectral width of 13 cm⁻¹. Since a time constant of 10 sec was used, a spectral slit width was covered in about ten time constants. Voltage measurements were made at 1.1-cm⁻¹ intervals. These studies were made with 4 Torr of Cl_2, 189 Torr of O_2, and 567 Torr of He. These reactants were photolyzed with square-wave radiation at 2 Hz. The cumulative results of 40 such scans are shown in Figure 2a as a plot of amplitude and phase of the modulated signal *vs.* infrared frequency. To test reproducibility, another set of 40 scans of the 1400–1520 cm⁻¹ region was recorded. The cumulative results of the second set are given in Figure 2b. The two sets of scans were then combined to obtain an improvement in signal-to-noise ratio. The combined results of 80 scans were curve-smoothed and corrected for background to obtain true absorbance. The resulting spectrum is shown in Figure 2c. Curve smoothing consisted of applying a simple three-point moving average to the raw data. Since a spectral slit width is covered by 12 data points, a three point average will not introduce distortion.

Another determination of this absorption was made with 4 Torr of Cl_2 and 756 Torr of O_2 with a 1-Hz flashing rate. The cumulative results of 40 scans were curve-smoothed, corrected for carrier intensity, and plotted in Figure 3. A comparison of Figures 2 and 3 shows that we have detected an absorbance between 1430 and 1470 cm⁻¹, but that the resolution is quite low. In particular the apparent peak in Figure 2 at 1470 cm⁻¹ is probably not a real feature.

Although a chemically modulated absorption spectrum that could be attributed to the ClO radical was not

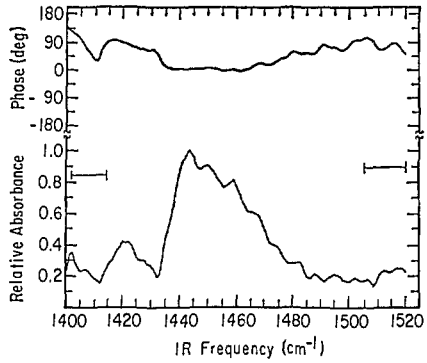

Figure 3. ClOO infrared molecular modulation spectrum observed with 4 Torr of Cl_2 and 756 Torr of O_2, 1-Hz square-wave ultraviolet photolysis, smoothed cumulative measurements, 40 scans. ⊢⊣ indicates spectral slit width.

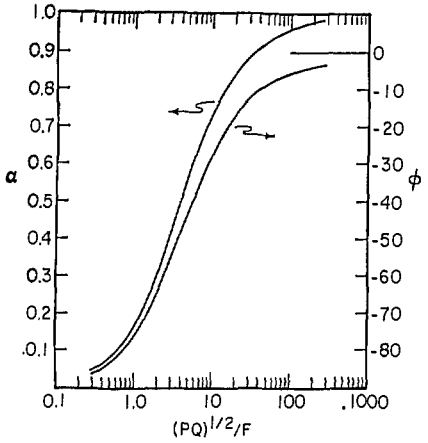

Figure 4. General curves for radical phase shift, ϕ, and relative modulation amplitude, $\alpha = A/A_s$, for a system where radicals are removed by a second-order process, eq 8, as a function of the dimensionless parameter given by eq 11.

detected in the exploratory spectroscopic measurements, attempts were made to observe its spectrum by means of multiple scanning over narrower spectral regions for longer periods of time. On the basis of Porter's[1] prediction of the ClO ground-state vibrational frequency (868 cm^{-1}), the observed frequencies (936, 945 cm^{-1}) of a matrix-isolated species tentatively identified as $(ClO)_2$ by Rochkind and Pimentel,[13] and the strong peak we previously observed[16a] between 930 and 980 cm^{-1}, it can be expected that the absorption band of ClO most probably lies in the region of 850–980 cm^{-1}. Therefore, this region was scanned extensively, over prolonged periods of time and under a variety of experimental conditions, in an effort to observe a modulated infrared absorption spectrum of ClO. However, these attempts proved fruitless, even under seemingly the most favorable conditions. The modulation reported previously[16a] as ClO is in fact not ClO but another species arising from a trace of CO impurity in the system. When we purposely add CO, a strong radical absorption centered at 940 cm^{-1} is seen. This species also gives absorptions at 1835 and 1905 cm^{-1}. The identity of this radical is not known at this time, and further work is underway.

The infrared spectrum of the Cl_2–O_2 or Cl_2–O_2–He system has been recorded over the region of 725–3000 cm^{-1}, both before and after reaction, for evidence of impurities in the reactants or formation of stable infrared-active products. No spectroscopically detectable reactive impurities have been observed in research grade Cl_2, ultrahigh purity O_2, or extra-dry O_2 after passage through a hydrocarbon combustion furnace. With respect to infrared-active reaction products, none has been detected with the exception of a small amount ($\sim 10^{13}$ molecules/cm^3) of phosgene that invariably forms and increases slowly with time in a closed cell. Since phosgene is formed even after prolonged pumping on the cell, or after chemical purging by prolonged photolysis of Cl_2 in the cell, it has been concluded that it arises from the slow reaction of Cl atoms with the organic coating on the interior surface of the cell, which undoubtedly serves as the source of the carbonyl in phosgene. The chemically modulated absorption spectrum of phosgene has not, however, been detected under these circumstances.

Kinetic Measurements. In this section we want to point out how the molecular modulation method gives kinetic data analogous in form and detail to standard kinetic methods that measure concentrations as a function of time. Analogies between this and previous methods will be pointed out. The expression "order with respect to time" refers to how the concentration of reactant changes with time throughout the course of a single experiment. Reactions may be first order, second order, fractional order, etc. The expression "order with respect to concentration" refers to how the initial reaction rate is affected by initial reactant concentrations for a series of separate experiments. In the molecular modulation method, it takes a long time (minutes to hours) to measure the phase shift and modulation amplitude for a given set of reactant concentrations and photolysis period (square-wave excitation). A series of measurements with the same reactant concentrations and at different periods of photolysis (that is, different flashing frequencies) gives data analogous to a single run in ordinary kinetics where concentrations are followed as a function of time.

For radicals destroyed by second-order kinetics

$$\underset{\text{in light}}{\frac{dx}{dt} = P - Qx^2} \qquad \underset{\text{in dark}}{\frac{dx}{dt} = -Qx^2} \tag{8}$$

the steady-state concentration of radicals is

$$x_s = (P/Q)^{1/2} \tag{9}$$

The half-time for disappearance of this concentration of radicals after the light is turned off is

$$t = (PQ)^{-1/2} \tag{10}$$

The relative modulation amplitude A/A_s and the phase shift φ between radical x and photolysis light have been shown[16b] to be given by a complicated function of the dimensionless parameter

$$\frac{(PQ)^{1/2}}{F} = \frac{T}{(PQ)^{-1/2}} = \frac{T}{t} = \frac{\text{period of photolysis cycle}}{\text{half-life of radical in the system}} \tag{11}$$

where T is the period (light cycle and dark cycle) of one cycle of photolysis light and F is the frequency of the photolyzing light.

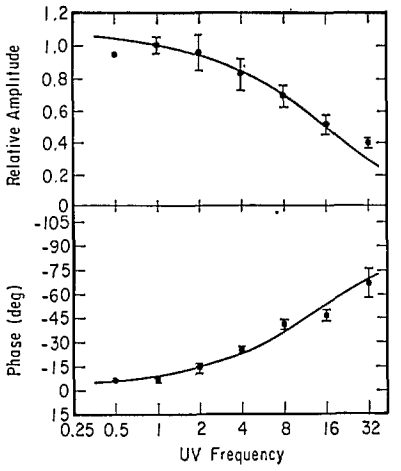

Figure 5. Mean values of infrared modulation phase and relative amplitude as a function of ultraviolet square-wave photolysis frequency, F, measured with 4 Torr of Cl_2 and 756 Torr of Cl_2, 298 °K.

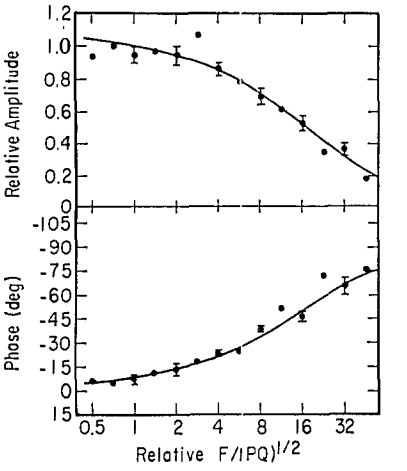

Figure 6. Same as Figure 5 except that all runs were normalized to the same reactant conditions as in Figure 5 by the relations given by eq 11 and 16.

For second-order destruction of radical, eq 8, a plot of relative modulation amplitude, $\alpha = A/A_s$, and phase shift, φ, against $(PQ)^{1/2}T$ is given by Figure 4. An actual set of data plotted as α or φ or both against log T would have the same shape as Figure 4 and by superimposing a master plot and sliding scales, the value of $(PQ)^{1/2}$ or the radical half-life can be evaluated. Figure 4 is analogous to a conventional plot of reactant against time for a given run.

A series of measurements was made at a fixed infrared frequency, 1443 cm^{-1}, corresponding to the maximum of the absorption band, at 6-mm slit widths, 72-m optical path length, RC filter time constant of 10 sec, with readings taken at 8-sec intervals, 4 Torr of Cl_2, and 756 Torr of O_2. Phase and amplitude of the modulated infrared system were measured at seven different ultraviolet, square-wave, flashing frequencies F: 0.5, 1.0, 2.0, 4.0, 8.0, 16, and 32 Hz. The average time for each run was 40 min. Results are given in Figure 5. Each plotted point is the average value of multiple determinations, and the error bars cover twice the standard deviation. The smooth curve is that for second-order destruction of radicals.[16c] The observed modulation amplitude by ClOO at 1 cps is

$$\Delta I/I_0 = 1.50 \times 10^{-4} \quad (12)$$

and the half-life of ClOO based on Figure 5 is

$$t = 0.0173 \text{ sec} \quad (13)$$

Another series of measurements was made in which O_2 was reduced by a factor of 4 and the system was brought up to 1 atm total pressure by addition of nitrogen: 4 Torr of Cl_2, 189 Torr of O_2, and 567 of Torr N_2. A similar analysis gave the half-life

$$t = 0.0341 \text{ sec} \quad (14)$$

A comparison of eq 13 and 14 indicates that the half-life is inversely proportional to the square root of oxygen concentration.

Experiments were also carried out at constant oxygen (1 atm) and varied amounts of Cl_2. The three runs, including that of eq 13 are summarized as

Cl_2, Torr	O_2, Torr	t, sec	$t[Cl_2]^{1/2}$, sec $Torr^{1/2}$
4	756	0.0173	0.035
2	758	0.0268	0.038
1	759	0.0285	0.029

These results show fairly large experimental error, but they are consistent with an inverse square root dependence of the half-life of ClOO on chlorine.

The results of all runs were normalized to the reference conditions, 4 Torr of Cl_2 and 756 Torr of O_2, on the basis that

$$PQ \propto [O_2][Cl_2] \quad (15)$$

$$[ClOO]_s^2 = (P/Q) \propto [O_2][Cl_2] \quad (16)$$

and all data from the four runs are plotted against flashing frequency in Figure 6. The half-life inferred from all data is 0.0156 sec and the modulation amplitude at 1.0 Hz is 1.50×10^{-4}. These results and the experimental conditions are summarized in Table I.

Table I. Summary of Primary Kinetic Data from Infrared and from Ultraviolet Studies at 298° K

Quantity, units	Values deduced from Ir	Values deduced from Uv
aI_0, sec^{-1}	0.80×10^{-3}	3.92×10^{-3}
$[Cl_2]$, particles/cc	13.00×10^{16}	3.80×10^{16}
$[O_2]$, particles/cc	2.45×10^{19}	2.45×10^{19}
L, cm	7200	326
A_2	1.50×10^{-4}	1.26×10^{-3}
t_2, sec	0.0156	0.0119
A_1		1.94×10^{-3}
t_1, sec		0.384

Ultraviolet Spectroscopic Measurements. Chlorine at 1.8 Torr in the presence of 1 atm of oxygen was photolyzed with square-wave excited lamps at 1 Hz. The rate of light absorption was estimated to be 2.4×10^{14} photons/(cm^3 sec). A modulation was observed at wavelengths between 2250 and 2900 Å, Figure 7. The measured phase angles lie in the quadrant expected for intermediates;[16a] however, the change in phase observed with wavelength indicates the presence

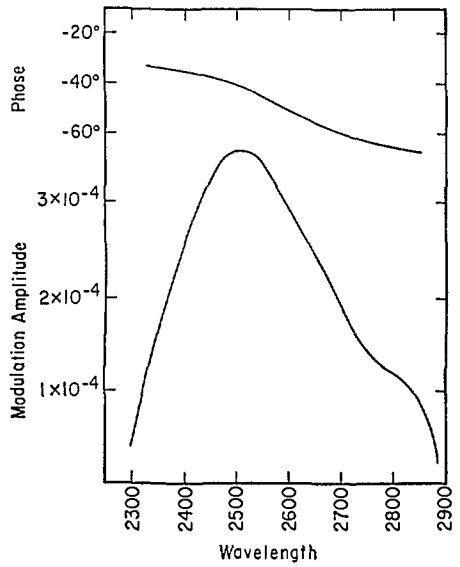

Figure 7. Modulation spectrum in the ultraviolet showing presence of two or more intermediates by virtue of a change of phase shift with wavelength; 1.8 Torr of Cl_2, 1 atm of O_2, 1 Hz square-wave photolysis.

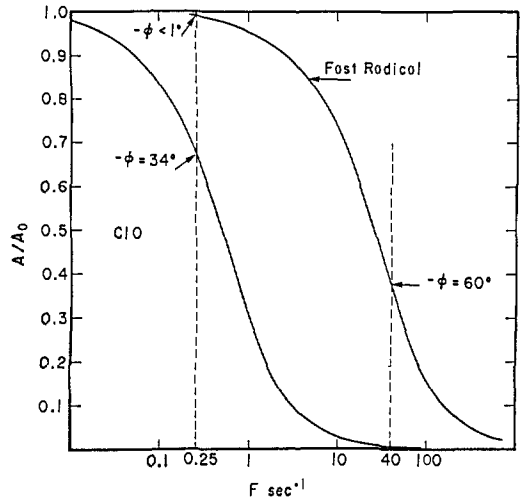

Figure 9. Calculated relative modulation amplitude for the two intermediates observed in this system (based on rate constants deduced later in this article; presented here to demonstrate how unwanted overlap of ClO can be reduced to zero at high frequencies, and how the phase of a fast radical can be reduced to a known zero value at low photolysis frequencies).

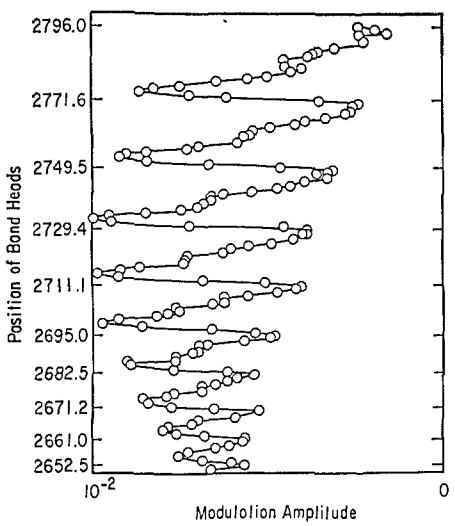

Figure 8. Relatively high resolution molecular modulation spectrum showing vibrational structure of ClO, compared to position of ClO band heads as found by Porter (ref 1); 4 Torr of Cl_2, 46 Torr of O_2, 0.25 Hz, spectral slit width 2 Å.

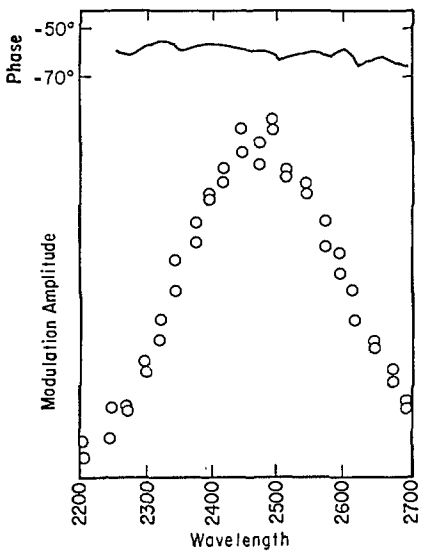

Figure 10. Spectrum of the new species taken at high frequency, 32 Hz (*cf.* Figure 9). The phase remains essentially constant with wavelength (contrast Figure 7).

of two or more species with overlapping absorption spectra. The small phase angle at 2300 Å represents a "fast" intermediate, that is, one whose lifetime is short compared to the flashing frequency of 1 Hz. The larger phase angle at 2800 Å indicates a much slower intermediate. The observed signal is a vector sum of the various species present.

Using literature values[1-3] for the rate of recombination of ClO and for its cross section,[11] we estimate that this species should be seen in the modulation experiment as a slow intermediate. From flash photolysis studies, ClO is known to have a banded structure from 3000 Å to the dissociation limit at 2630 Å. Porter[1] has published the locations of the vibrational band heads in this region. Experimentally it was found that reducing the total pressure to 50 Torr and flashing at 0.25 Hz increased the modulation amplitude. This allowed the spectral slit width to be reduced from 13 to 2 Å. Figure 8 shows the experimentally observed modulation amplitude together with the positions of the ClO band heads as determined by Porter. The two are in excellent agreement. Thus one of the species being observed is definitely identified as the ClO radical.

It was desired to obtain a spectrum of the fast intermediate with a minimum of interference from ClO. Since ClO is a slow intermediate, its modulation amplitude can be suppressed by increasing the flashing frequency of the photolyzing radiation. As can be seen from Figure 9, the amplitude of ClO modulation begins to fall off at a lower frequency than does the unknown, because of the difference in lifetimes. If the flashing frequency is chosen approximately equal to the lifetime of the fast intermediate, this is much faster than the ClO lifetime. A spectrum taken at 32 Hz is given in

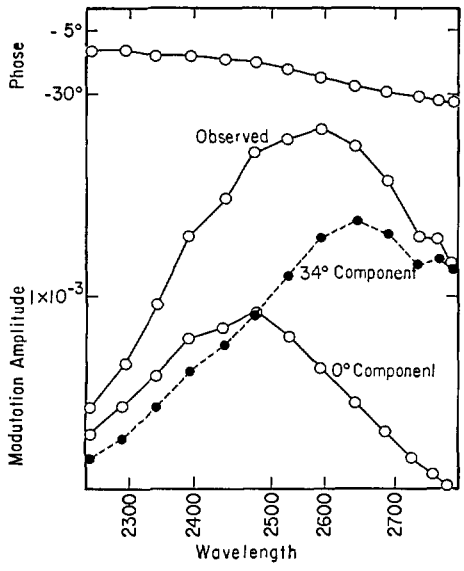

Figure 11. Resolution of the complex spectrum into two components of constant phase at low (0.25 Hz) photolysis frequency (*cf.* Figure 9). The 34° component has been identified as ClO (*cf.* Figure 8).

Figure 10. The modulation spectrum extends from 2250 to 2700 Å with a maximum about 2475 Å. The phase angle is almost constant (−60 to −65°) over this range, indicating ClO modulation was effectively suppressed.

At lower frequencies the modulation is no longer simple but a vector sum of several amplitudes and phases. If this complex spectrum consists of only two species and if the phase of each is known, then the complex modulation spectrum can be factored into two components. An experiment was carried out at 0.25 Hz, Figure 11. The observed modulation shows a maximum at 2600 Å and the phase angle varies from −12° at 2300 Å to −34° at 2800 Å. From Figure 9 it can be seen that if an intermediate has a phase of −60° at 32 Hz, it would have essentially zero phase angle at 0.25 Hz. If the fast intermediate has zero phase, and the plateau of −34° at 2800 Å is taken as the phase of ClO, then the observed amplitude can be decomposed into two separate spectra, one for ClO and one for the faster species, Figure 11.

The two methods of deducing the spectrum of the fast intermediate are compared in Figure 12, where the results have been normalized at 2500 Å. The two determinations agree within experimental error. This would indicate that the assumption of only two intermediates is correct, and that the phase of ClO is close to −34°.

The new intermediate has a broad unstructured absorption between 2300 and 2600 Å, and the spectrum alone does not give any evidence as to the identity of the species. The identity of this absorption is deduced from kinetic data in the next section.

Kinetic Measurements. Between 2200 and 2800 Å the shapes of the absorption spectra of two intermediates in the chlorine–oxygen system have been determined. One of these is the free radical ClO. It will be shown later that if the other is ClOO, then the system should obey the coupled differential equations

$$\begin{aligned} \mathrm{d[ClOO]}/\mathrm{d}t &= P - Q[\mathrm{ClOO}]^2 \\ \mathrm{d[ClO]}\,\mathrm{d}t &= R[\mathrm{ClOO}]^2 - S[\mathrm{ClO}]^2 \end{aligned} \tag{17}$$

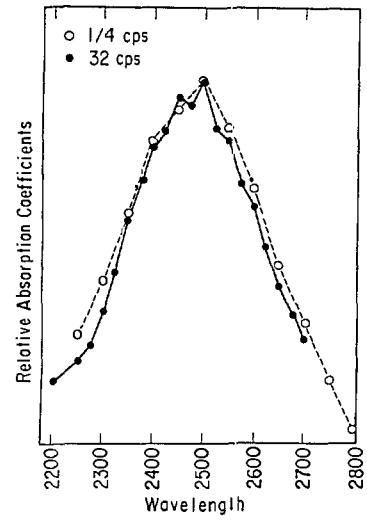

Figure 12. Comparison of the two methods (Figures 10 and 11) of determining the spectrum of the new species.

where P, Q, R, and S may depend on variables such as $[O_2]$, $[Cl_2]$, I_0, and $[M]$. Quantitative interpretation of data requires solution of these coupled equations by means of a computer program. However, for purposes of discussion it is very convenient to consider an approximation, which is valid only at very low flashing frequencies. The steady-state concentration of ClOO is

$$[\mathrm{ClOO}]_s = (P/Q)^{1/2} \tag{18}$$

The radical ClOO is much faster than ClO, and so we make the "steady-state assumption" for ClOO relative to ClO. In this case the differential equations are

$$\begin{aligned} \mathrm{d[ClOO]}/\mathrm{d}t &= P - Q[\mathrm{ClOO}]^2 \\ \mathrm{d[ClO]}/\mathrm{d}t &= RP/Q - S[\mathrm{ClO}]^2 \end{aligned} \tag{19}$$

The symbol A is used for amplitude, t for half-life, and $\sigma(\lambda)$ for absolute cross section for light absorption at the wavelength λ. The subscript 2 refers to ClOO and the subscript 1 refers to ClO. Under low-frequency conditions the amplitudes and half-lives in terms of the rate parameters of eq 17 and 19 are

$$t_2 = (PQ)^{-1/2} \tag{20}$$

$$A_2 = \Delta I_2/I_0 = \sigma_2(\lambda)L(P/Q)^{1/2} \tag{21}$$

$$t_1 = (PRS/Q)^{-1/2} \tag{22}$$

$$A_1 = \Delta I_1/I_0 = \sigma_1(\lambda)L(PR/QS)^{1/2} \tag{23}$$

where I is measuring light intensity and L is the optical path length. Except where noted otherwise, the individual terms P, Q, R, and S were evaluated from observed phases and amplitudes by means of a computer program; but the data are summarized and presented in terms of the quantities, eq 20–23, which have the definite physical interpretations at low photolysis frequencies.

For one set of reactant conditions, 1.17 Torr of Cl_2 and 759 Torr of O_2, the complete spectrum of ClO and ClOO was scanned at each of the frequencies 0.25, 0.50, 1, 2, 4, 8, 16, and 32 Hz. The observed ClOO phase is plotted against flashing frequency in Figure 13. The solid curve is calculated on the assumption that the half-

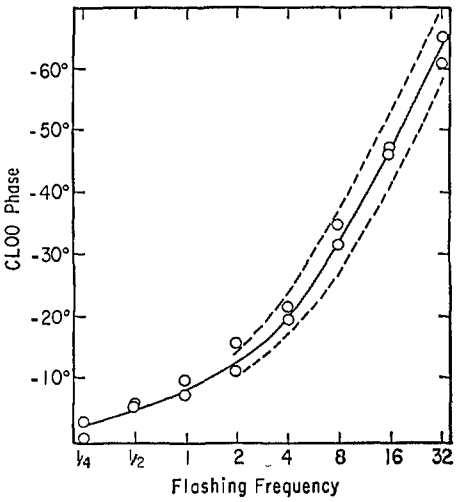

Figure 13. Observed phase of ClOO as a function of the flashing frequency, with three curves calculated on the assumption of various half-lives of ClOO in the system: solid curve, 0.0119 sec; dotted curves, 0.0096 and 0.0154 sec.

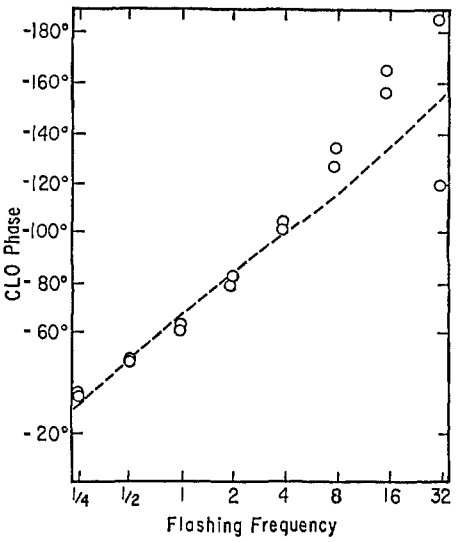

Figure 14. Observed phase of ClO as a function of the flashing frequency, with a curve fitted to the half-life of ClO and the known half-life of ClOO: $t_1 = 0.384$ sec, $t_2 = 0.0119$ sec.

time of ClOO is 0.0119 sec; the dashed curves are calculated from half-times of 0.0096 and 0.0154 sec. The experimental points indicate that the half-time is

$$t_2 = 0.0119 \pm 0.0015 \text{ sec} \quad (24)$$

Under these conditions the observed modulation amplitude at low frequency and at 2500 Å is

$$A_2 = 1.26 \times 10^{-3} \quad (25)$$

The phase of ClO as a function of flashing frequency is found by solving the simultaneous differential eq 17. The observed phases of ClO are plotted as a function of flashing frequency in Figure 14. It is notable that the observed and calculated phases of ClO go beyond −90° into what is normally[16a] considered the product quadrant. However, this behavior follows from ClO being a secondary radical. At frequencies where ClOO has a significant phase shift, the additional phase shift or time lag pushes ClO past −90°. As an experimental observation, this behavior is diagnostic of the "generation" of the radical under observation; that is, primary, secondary, or later. The shape of the observed phase shift *vs.* frequency curve is in good agreement with the theoretical form, Figure 14, although the phases are poorly determined at high frequencies where the amplitude is very low. The calculated curve is based on t_2 being 0.0119 sec, eq 24, and on the following half-life of ClO.

$$t_1 = 0.384 \text{ sec} \quad (26)$$

The observed modulation amplitude at 2700 Å is

$$A_1 = 1.94 \times 10^{-3} \quad (27)$$

The experimental conditions and the four data, eq 24–27, are summarized in Table I. Figures 13 and 14 are analogous to conventional kinetic plots of concentrations *vs.* time during the course of one run. To find "order with respect to concentration," a series of runs must be made for different initial conditions.

At low flashing frequency, 0.25 Hz, the phase lag of ClOO is very nearly zero, so that the measured modulation gives a direct measure of $(P/Q)^{1/2}\sigma_2$. A series of runs was made at an oxygen pressure of 1 atm with Cl_2 from 0.5 to 2.8 Torr. The modulation amplitude and Cl_2 partial pressures are listed in Table II. A plot of log amplitude against log $[Cl_2]$ gives an empirical order of 0.42 which is fairly close to the expected value of 0.5. In Table II the observed modulation amplitude is divided by $[Cl_2]^{1/2}$ and the optical path length L. Except for the highest Cl_2 pressure, the variation in amplitude is well given by $[Cl_2]^{1/2}$.

Table II. The Effect of Cl_2 on the Steady-State Concentration of ClOO as Observed from Modulation Amplitude in the Ultraviolet at 2500 Å[a]

Cl_2, Torr	10^3A_2	$10^{14}A_2/L[Cl_2]^{1/2}$, cm^{-1} (cc/particle)$^{1/2}$
0.49	0.74	1.80
	0.76	1.85
	0.74	1.80
	0.73	1.77
	0.73	1.77
	0.76	1.85
	0.71	1.72
0.82	0.89	1.67
	0.86	1.62
	0.88	1.65
	0.88	1.65
1.37	1.21	1.76
	1.18	1.71
	1.16	1.69
2.85	1.44	1.45
	1.47	1.48
	1.47	1.48

[a] Oxygen pressure constant at 1 atm.

Another set of conditions was selected to give a sensitive test of the order of the steady-state concentration of ClO with respect to Cl_2. Even at the lowest frequency used here (0.25 Hz) the ClO phase shift is about −30°. However, the phase can be used to extrapolate the measured amplitude to the low-frequency limit, giving a measure of $(PR/QS)^{1/2}\sigma_1$. The observations are listed in Table III. The empirical order is 0.53, very close to the expected value of 0.50. The observed

amplitudes are normalized in Table III with $[Cl_2]^{1/2}$. These studies show that both $(P/Q)^{1/2}$ and $(PR/QS)^{1/2}$ vary as the square root of $[Cl_2]$, and thus the ratio (R/S) is independent of chlorine. From the proposed mechanism, the role of chlorine in each case is to absorb radiation and dissociate to atoms. These observations confirm this effect and find no other role of Cl_2 in the system.

Table III. The Effect of Cl_2 on the Steady-State Concentration of ClO as Observed from the Modulation Amplitude in the Ultraviolet at 2700 Å[a]

Cl_2, Torr	10^3A_1, extrapolated to DC	$10^{14}A_1/L[Cl_2]^{1/2}$, cm^{-1} (cc/particle)$^{1/2}$
2.5	3.90	4.20
	3.75	4.03
	3.85	4.14
	3.85	4.14
6.7	6.57	4.32
	6.40	4.20
	6.42	4.22
	6.45	4.24
2.6	3.97	4.19
	3.83	4.04
	3.88	4.10
	3.83	4.04
6.9	6.54	4.23
	6.42	4.16
	6.44	4.17
	6.47	4.19

[a] Oxygen pressure constant at 1 atm.

The effect of oxygen on the steady-state concentration of ClOO was determined in a series of pairs of experiments. However, as oxygen is reduced, the ratio ClOO/ClO is also reduced. Because of the overlap of spectra it becomes difficult to get a good measurement of ClOO over a wide range of oxygen pressure. The results of these experiments are presented in Table IV.

Table IV. The Effect of O_2 on the Steady-State Concentration of ClOO and of ClO

$10^{16}[Cl_2]$, particles/cc	$10^{19}[O_2]$, particles/cc	Relative ClOO		Relative ClO	
		Obsd	Calcd[a]	Obsd	Calcd[b]
1.65	2.45	1.01	1.00	1.02	1.00
		0.99		0.98	
1.65	1.22	0.71	0.71	0.98	1.00
		0.66		0.98	
0.82	2.45	0.71	0.71	0.71	0.71

[a] Calculated by dividing by $[O_2]^{1/2}[Cl_2]^{1/2}$. [b] Calculated by dividing by $[O_2]^0[Cl_2]^{1/2}$.

It can be seen that ClOO, or the constant $(P/Q)^{1/2}$, varies as the square root of oxygen pressure.

$$[ClOO]_s = (P/Q)^{1/2} \propto (Cl_2)^{1/2}(O_2)^{1/2} \qquad (28)$$

The effect on [ClO] of varying O_2 from 1 atm to 0.50 atm at constant Cl_2 was studied. These results are also shown in Table IV. At this range of pressures, the steady-state concentration of ClO is independent of oxygen (with very small amounts of oxygen and large inert gas pressure, the steady-state concentration of ClO does become dependent on oxygen as the reaction Cl + Cl + M → Cl_2 + M becomes important). The dependence of the concentration of ClO on reactant variables is thus found to be

$$[ClO]_s = (PR/QS)^{1/2} \propto (Cl_2)^{1/2}(O_2)^0 \qquad (29)$$

Our observed infrared absorption band at 1443 cm^{-1} coincides with one of the fundamental bands of ClOO as observed in a matrix by Arkell and Schwager.[15] The lifetime of ClOO in the infrared varied with O_2 and with Cl_2 in the same manner as did the lifetime of the "fast species" in the ultraviolet. These lifetimes can be compared on a quantitative basis by correcting each system for its light intensity and concentration of Cl_2 and O_2. From the ultraviolet measurements we have

$$t_2(aI_0[Cl_2][O_2])^{1/2} = 1.38 \times 10^{-15} \text{ cc/(particlesec}^{1/2}) \qquad (30)$$

From the infrared measurements we have

$$t_2(aI_0[Cl_2][O_2])^{1/2} = 1.27 \times 10^{-15} \text{ cc/(particle sec}^{1/2}) \qquad (31)$$

Within experimental error these two kinetic data are in agreement. Thus this combination of spectroscopic and kinetic data identifies the new species observed in the ultraviolet, Figure 12, as the peroxyl free radical ClOO. For the remainder of this article, the species whose absorption spectra are given by Figure 3 (infrared) and Figure 12 (ultraviolet) will be regarded as the radical ClOO.

The effect of a foreign gas M on the kinetics of the ClOO radical is best demonstrated by selecting conditions where the phase shift is about 45°. Then a measure of the phase gives $(PQ)^{1/2}$ and a measure of the amplitude gives $\sigma_2L(P/Q)^{1/2}$. The ratio gives Q/σ_2L. The results are given in Table V. It can be seen that the rate constant Q for disappearance of ClOO does not depend on inert gas M.

Table V. The Effect of Inert Gas M on the Kinetics of ClOO Disappearance

Cl_2, Torr	O_2, Torr	Ar, Torr	Phase, deg	$\Delta I/LI_0$, cm^{-1}	Q/σ_2, cm (particle sec)$^{-1}$
1.7	150	0	−27.3	1.60×10^{-6}	1.2×10^7
1.7	150	608	−31.6	1.25×10^{-6}	1.2×10^7

The effect of foreign gas M on ClO kinetics is best studied by selecting conditions where the ClOO phase shift is close to zero and where the ClO phase shift is finite and easily measured, about −30° (*cf.* Figure 9). Then a measurement of phase gives $(PRS/Q)^{1/2}$ and a measurement of modulation amplitude gives $(PR/QS)^{1/2}\sigma_1L$. The ratio of these two observed terms is simply S/σ_1L. From eq 17 it may be noted that S is the empirical rate constant for the second-order destruction of ClO radicals. A series of runs was made at constant Cl_2, O_2, and I_0, but with various added amounts of argon. Observation of ClO was made at 2577 Å, which is in the continuum region of ClO absorption. (In the banded region at 2700 Å there might be some inert gas effect from pressure broadening, but in the continuum at 2577 Å such an effect is not to be expected.) The observed quantity S/σ_1 (corrected for the small nonzero value of the phase and amplitude of ClOO as calculated from the parameters P and Q previously determined) as a function of added Ar is given in Table VI. It is noteworthy that at constant Cl_2 and O_2, the rate of destruction of ClO is increased by added argon. Thus contrary to the indications obtained by Porter and co-

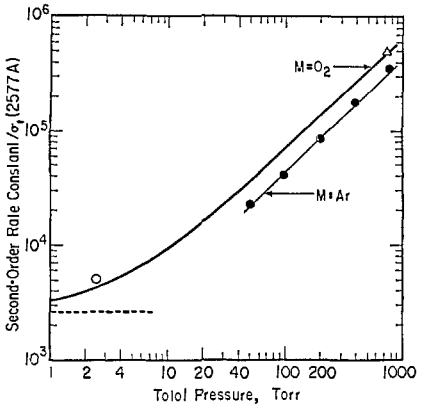

Figure 15. The empirical second-order rate constant for the destruction of ClO as a function of total pressure. From the mechanism the constant is $2(e + iK_3[M])/\sigma_1(2577)$. The heavy solid curve is calculated on the basis of e of Table IX and with M = O_2, where $iK_3 = 5.0 \times 10^{-32}$ cc²/(particle² sec): light solid curve, M = Ar, $iK_3 = 3.3 \times 10^{-32}$ cc²/(particle² sec). The dotted line is given by $e = 6.3 \times 10^{-15}$ cc/(particle sec). ○, experimental point by Clyne and Coxon (ref 11); △, experimental point, this study, Table I; ●, experimental points with added argon, this study, Table VI.

workers, there is a strong foreign gas effect in this system. To test for the order of the empirical rate parameter S with respect to total gas concentration

$$[M] = [Cl_2] + [O_2] + [Ar] \quad (32)$$

the results are plotted as log S/σ_1 *vs.* log [M] in Figure 15. Included on this figure is the value of S/σ_1 by

Table VI. The Effect of Inert Gas M on the Kinetics of ClO Disappearance

Cl_2, Torr	O_2, Torr	Ar, Torr	Second-order rate constant, $10^{-8}S/\sigma_1$(2577 Å)			
3	27	20	24.0	24.0	23.6	23.4
			22.2	22.4	22.9	22.9
3	27	70	40.0	39.7	39.6	39.6
			41.0	39.7	39.2	39.4
3	27	170	81.0	80.9	80.2	80.7
			84.0	80.9	80.0	80.7
3	27	370	185	178	181	184
			185	178	176	178
3	27	730	346	342	361	371
			364	351	365	371

Clyne and Coxon at a total pressure of about 1–2 Torr. The calculated curve on this figure is of the form

$$S = S' + S''[M] \quad (33)$$

The evaluation of the parameters S' and S'' is described in the Discussion section below. The plot of log S/σ_1 against log [Ar] has unit slope between 50 and 750 Torr, and the constant S, second order with respect to time, is first order with respect to chaperon gas M.

Discussion

Mechanism. For convenient reference the entire mechanism is written here.

$$Cl_2 + h\nu \xrightarrow{a} Cl + Cl \qquad \text{rate} = aI_0[Cl_2] \quad (34)$$

$$Cl + O_2 + M \underset{c}{\overset{b}{\rightleftharpoons}} ClOO + M \qquad K_1 = \frac{b}{c} = \frac{[ClOO]}{[Cl][O_2]}$$

$$Cl + ClOO \underset{e}{\overset{d}{\rightleftharpoons}} ClO + ClO \qquad K_2 = \frac{d}{e} = \frac{[ClO]^2}{[Cl][ClOO]}$$

$$Cl + ClOO \xrightarrow{f} Cl_2 + O_2$$

$$ClO + ClO + M \underset{h}{\overset{g}{\rightleftharpoons}} Cl_2O_2 + M \qquad K_3 = \frac{g}{h} = \frac{[Cl_2O_2]}{[ClO]^2}$$

$$Cl_2O_2 + M \xrightarrow{i} Cl_2 + O_2 + M$$

$$Cl + Cl + M \xrightarrow{j} Cl_2 + M$$

There are ten elementary reactions, a–j, and four intermediates, Cl, ClOO, ClO, and Cl_2O_2. The introductory section gave a brief history and key references to the source of these various steps. The principal contributions of this present work are to observe the free radical ClOO in the gas phase by both infrared and ultraviolet absorption spectroscopy and to demonstrate the complex inert gas dependent nature of the second-order disappearance of the ClO radical. Clyne and Coxon assumed that there was a "chaperon gas" effect at higher pressures to explain their very anomalously low rate constant for ClO disappearance, but they did not realize it was a linear function (compare eq 33) from a few Torr to 1 atm and presumably higher.

In the usual analysis of complex mechanisms one makes the steady-state assumption for the free-radical intermediates. Such a procedure is totally unacceptable here, since it is precisely the rate of formation and decay of these radicals that we measure. One must solve the full set of differential equations to calculate the expected phase and amplitude of a modulated signal. Because the rate of radical change is often the difference between two large numbers, one must be extremely careful in making any assumptions. The approximations we do make in simplifying the rate expressions will be explicity identified.

The problem of the ClOO radical is most conveniently solved if we formulate the differential rate equation, not for Cl and ClOO separately, but for their sum.

$$\frac{d([ClOO] + [Cl])}{dt} = 2aI_0[Cl_2] - 2(d + f)[Cl][ClOO] + 2e[ClO]^2 - 2j[Cl]^2[M] \quad (35)$$

We assume that Cl and ClOO are in chemical equilibrium through reactions b and c, and we solve for the chlorine atom concentration

$$[Cl] = [ClOO]/K_1[O_2] \quad (36)$$

With this relation for [Cl], eq 35 becomes

$$\frac{d[ClOO]}{dt} = \left\{\frac{aI_0[Cl_2] + e[ClO]^2}{1 + K_1[O_2]}\right\}2K_1[O_2] - (d + f) + \frac{j[M]}{K_1[O_2]}\frac{2[ClOO]^2}{1 + K_1[O_2]} \quad (37)$$

We make the simplifying assumption (to be verified later) that

$$e[ClO]^2 \ll aI_0[Cl_2] \quad (38)$$

In this way we obtain a differential equation for ClOO having the form of eq 8 or eq 17.

$$\frac{d[ClOO]}{dt} = \frac{2aI_0[Cl_2]K_1[O_2]}{1 + K_1[O_2]} - \frac{2}{1 + K_1[O_2]}\left\{(d + f) + \frac{j[M]}{K_1[O_2]}\right\}[ClOO]^2 \quad (39)$$

In terms of eq 8 and 17 the empirical rate parameters P and Q are given by the mechanism as

$$P = \frac{2aI_0[Cl_2]K_1[O_2]}{1 + K_1[O_2]} \quad (40)$$

$$Q = \frac{\{2(d + f) + j[M]/K_1[O_2]\}}{1 + K_1[O_2]} \quad (41)$$

It was shown in Table V that the rate constant Q was not changed by adding 608 Torr of Ar to a reaction mixture of 1.7 Torr of Cl_2 and 150 Torr of O_2. Thus it is reasonable to make the assumption

$$j[M]/K_1[O_2] \ll (d + f) \quad (42)$$

and thus eq 41 simplifies to

$$Q = \frac{2(d + f)}{1 + K_1[O_2]} \quad (43)$$

It will be shown later that this simplification is valid in systems that contain only Cl_2 and O_2, with O_2 in excess. However, in cases where an inert gas M is in large excess over O_2, eq 42 is no longer valid, but then it is quite simple to use eq 41.

The problem for ClO is most readily solved if we formulate the differential equation for the sum ([ClO] + 2[Cl_2O_2]) rather than for each species separately.

$$\frac{d([ClO] + 2[Cl_2O_2])}{dt} = 2d[Cl][ClOO] - 2e[ClO]^2 - 2i[M][Cl_2O_2] \quad (44a)$$

In this equation we replace Cl and Cl_2O_2 by

$$[Cl] = [ClOO]/K_1[O_2], \quad [Cl_2O_2] = K_3[ClO]^2 \quad (44b)$$

to obtain the expression

$$(1 + 4K_3[ClO])\frac{d[ClO]}{dt} = \frac{2d[ClOO]^2}{K_1[O_2]} - (2e + 2iK_3[M])[ClO]^2 \quad (44c)$$

We now make the assumption that

$$[ClO] \gg [Cl_2O_2] \text{ which implies } 4K_3[ClO] \ll 1 \quad (45)$$

The expression for the ClO radical now assumes the form of eq 17.

$$\frac{d[ClO]}{dt} = \frac{2d[ClOO]^2}{K_1[O_2]} - (2e + 2iK_3[M])[ClO]^2 \quad (46)$$

Under conditions of slow flashing frequency, the steady-state assumption may be made for ClOO, even though it may not be so made for ClO. The steady-state concentration of ClOO is

$$[ClOO]_s^2 = \frac{aI_0[Cl_2]K_1[O_2]}{d + f} \quad (47)$$

and to this approximation the rate equation for ClO takes the form of eq 19.

$$\frac{d[ClO]}{dt} \backsimeq \frac{2daI_0[Cl_2]}{d + f} - (2e + 2iK_3[M])[ClO]^2 \quad (48)$$

In terms of the empirical rate parameters of eq 19, the mechanism gives

$$R = \frac{2d}{K_1[O_2]} \quad (49)$$

$$S = 2(e + iK_3[M]) \quad (50)$$

The next stage of the argument is to write expressions for the four observables in terms of the parameters of the mechanism. The four observables are the two modulation amplitudes, A_2 and A_1, and the two half-lives, t_2 and t_1. The relation of these observables to the empirical rate parameters of eq 17, P, Q, R, and S, was given by eq 20–23. The relation of these parameters to the mechanism was given by eq 40, 41 (or 43), 49, and 50. Thus the relations of the four observables to parameters of the mechanism are

$$A_2 = \Delta I_2/I_0 = \sigma_2(\lambda)L\left(\frac{aI_0[Cl_2]K_1[O_2]}{d + f}\right)^{1/2} \quad (51)$$

$$t_2 = \{4aI_0[Cl_2]K_1[O_2](d + f)\}^{-1/2}(1 + K_1[O_2]) \quad (52)$$

$$A_1 = \sigma_1(\lambda)L\left(\frac{aI_0[Cl_2]}{e + iK_3[M]}\frac{d}{d + f}\right)^{1/2} \quad (53)$$

$$t_1 = \{4aI_0[Cl_2]d(e + iK_3[M])/(d + f)\}^{-1/2} \quad (54)$$

As shown below, these complex rate expressions can be solved for several of the elementary rate constants.

Constants from the Literature and from Thermodynamics. The absolute cross section for absorption of ultraviolet radiation by ClO has been determined several times, and we take the determination at 2577 Å by Clyne and Coxon[11] as the basic datum here. (This reference modifies an earlier paper by the same authors. In view of the earlier paper, the wavelength given in ref 11 as 2557 Å must be a misprint.) With this number setting the absolute scale and with our determination of the shape of the ClO absorption, we obtain the cross section for ClO as a function of wavelength $\sigma_1(\lambda)$ as given in Table VII. In order to calculate elementary rate constants from the data in Table VI, we need the value of this cross section at 2577 Å, which is

$$\sigma_1(2577 \text{ Å}) = 4.83 \times 10^{-18} \text{ cm}^2 \quad (55)$$

Table VII. Absolute Cross Section[a] for Absorption of Ultraviolet Radiation by the Free Radical ClOO and ClO in Units of 10^{-18} cm^2

λ, Å	ClOO, $\sigma_2(\lambda)$	ClO, $\sigma_1(\lambda)$[c]
2250	2.60	0.641
2300	4.91	0.846
2350	7.80	1.33
2400	10.5	1.91
2450	12.7	2.67
2500	13.3[b]	3.56
2550	12.4	4.45
2600	10.0	5.27
2650	7.28	5.68
2700	5.11	5.60
2750	3.40	4.85
2800	2.28	4.71

[a] $-d \ln I = \sigma[X]L$, where concentrations are in particle/cc, L is path length in cm, and ln is logarithm to base e. [b] This work, eq 64. [c] Based on 4.83×10^{-18} cm^2 at 2577 Å by Clyne and Coxon.[11]

The thermodynamic properties of ClOO and ClO can be fairly reliably inferred from the literature and from

this study. Durie and Ramsay[8] determined the dissociation energy of ground-state ClO by spectroscopic methods, from which one calculates the standard heat of formation of ClO at 298°K to be 24.6 kcal/mole. Carrington, Dyer, and Levy[21] observed the electron resonance spectrum of the ClO radical in the gas phase. As a result of their theoretical analysis they obtained values for the fine-structure constant ($A = 282 \pm 9$ cm^{-1}) and for the isotopic rotational constants ($B_0 = 0.622 \pm 0.01$ cm^{-1} for $^{35}Cl^{16}O$ and $B_0 = 0.611 \pm 0.001$ cm^{-1} for $^{37}Cl^{16}O$). Since the uncertainty in the vibrational frequency of ClO, 900 ± 100 cm^{-1}, has negligible effect, all parameters are available to calculate the entropy to the rigid-rotator harmonic-oscillator approximation. Our value is 52.4 cal $mole^{-1}$ deg^{-1}, 0.5 eu lower than that calculated from older data by Clyne and Coxon.[7] The thermodynamic properties of ClOO are largely inferred from kinetic data. Clyne and Coxon[11] measured the activation energy of reaction e and found it to be 2.5 ± 0.3 kcal/mole. From the observed rate constant for reaction d in this study (see below) and from the preexponential factor, which we estimated theoretically by approximate[22] methods, we find that the activation energy for reaction d must be close to zero. In this way the standard heat of formation of ClOO is estimated to be 22.8 kcal/mole. Since the fundamental frequencies of the ClOO radical[15] have been determined recently and its geometrical structure fixed fairly reliably, it is possible to make a better estimate of the absolute entropy of ClOO than that derived by Benson and Buss.[10] In the rigid-rotator harmonic-oscillator approximation, the standard entropy of ClOO at 298° is calculated to be 63.0 cal $mole^{-1}$ deg^{-1}. The thermodynamic properties of species in this system are summarized in Table VIII. From those thermodynamic values, we calculate the following equilibrium constants at 298°K

Table VIII. Standard Thermodynamic Properties at 298°K

	$S°_{298}$, cal/(mole deg)	$\Delta_f H°_{298}$, kcal/mole
O_2	49.0	0
Cl	39.5	29.0
ClO	52.4	24.6
ClOO	63.0	22.8
Cl_2	53.3	0

$$K_1 = 0.089 \text{ atm}^{-1} = 3.64 \times 10^{-21} \text{ cc/particle} \quad (56)$$

$$K_2 = 227 \quad (57)$$

The rate constant j for recombination of chlorine atoms has been reported by Hutton and Wright[23]

$$j = 1.17 \times 10^{-32} \text{ cc}^2/(\text{particle}^2 \text{ sec}) \quad (58)$$

where Ar is the "chaperon gas." Porter and Wright[3] observed that the overall recombination of chlorine atoms in oxygen was 46 times faster than the recombination of chlorine atoms in nitrogen. If this enhanced rate is ascribed to chemical reactions, by way of ClOO and ClO, this result implies

$$K_1(d + f) = 46j = 5.4 \times 10^{-31} \text{ cc}^2/(\text{particle}^2 \text{ sec}) \quad (59)$$

if one assumes the Cl atom recombination rate constant in Ar and N_2 to be the same. A recent article by Nicholas and Norrish[24] made an independent measurement of the rate constant b.

$$b = 1.7 \times 10^{-33} \text{ cc}^2/(\text{particle}^2 \text{ sec}) \quad (60)$$

Evaluation of Rate Constants from the Mechanism Using Ultraviolet Data. A particular set of reactant concentrations and light intensity was used to obtain values of the four observable quantities, A_2, t_2, A_1, and t_1; and the numerical values of reactant concentrations, rate of light absorption aI_0, and these quantities are given in Table I. These quantities will be combined with each other and then combined with quantities obtained from the literature or from thermodynamics, eq 55–60, in order to evaluate elementary rate constants of the mechanism.

Starting with eq 52, we square the half-life of ClOO, rearrange terms, and assign numerical values from Table I

$$\frac{1}{t_2{}^2 4aI_0[Cl_2][O_2]} = \frac{K_1(d+f)}{(1 + K_1[O_2])^2} = 4.82 \times 10^{-31} \text{ cc}^2/(\text{particle}^2 \text{ sec}) \quad (61)$$

The value of the equilibrium constant K_1 was estimated from thermodynamics, eq 56. This term appears weakly in the denominator of eq 61, and we find essentially directly from observed data

$$K_1(d + f) = 5.72 \times 10^{-31} \text{ cc}^2/(\text{particle}^2 \text{ sec}) \quad (62)$$

This value agrees reasonably well with that observed by Porter and Wright, eq 59. This expression may be solved for the sum of rate constants by dividing through with the thermodynamic value of K_1

$$(d + f) = 1.57 \times 10^{-10} \text{ cc/(particle sec)} \quad (63)$$

The expression for the modulation amplitude, eq 51, contains the known rate of light absorption, aI_0, the reactant concentrations, the constant K_1, the optical path length L, and the sum, $d + f$, just evaluated as eq 63. Thus a measured modulation amplitude, Table I, gives the absolute cross section for light absorption by ClOO at 2500 Å

$$\sigma_2(2500 \text{ Å}) = \frac{A_2}{L}\left(\frac{d+f}{aI_0[Cl_2]K_1[O_2]}\right)^{1/2} = 1.33 \times 10^{-17} \text{ cm}^2 \quad (64)$$

The observed half-life and modulation amplitude of ClO, eq 53 and 54, can be combined, together with the known value of the rate of light absorption and the cross section for ultraviolet light absorption of ClO as found by Clyne and Coxon, eq 55, to give the ratio of rate constants

$$\frac{d+f}{d} = \sigma_1(2700 \text{ Å})L(2aI_0[Cl_2])\frac{t_1}{A_1} = 109 \quad (65)$$

The value of $d + f$ was found in eq 63, and thus the

(21) A. Carrington, P. N. Dyer, and D. H. Levy, *J. Chem. Phys.*, 47, 1756 (1967).
(22) D. R. Herschbach, H. S. Johnston, K. S. Pitzer, and R. E. Powell, *ibid.*, 25, 736 (1956).
(23) E. Hutton and M. Wright, *Trans. Faraday Soc.*, 61, 78 (1965).
(24) J. E. Nicholas and R. G. W. Norrish, *Proc. Roy. Soc., Ser. A*, 307, 391 (1968).

Table IX. Summary of Rate Constants and Other Quantities Evaluated from the Observed Data and the Mechanism, 298°K

Quantity	Units	Uv	Ir	Other	Ref
a	cm^2	9.35×10^{-20}	9.35×10^{-20}		
I_0	photons/(cm^2 sec)	4.2×10^{16}	0.85×10^{16}		
aI_0	sec^{-1}	3.92×10^{-3}	0.80×10^{-3}		
K_1	cc/particle			3.62×10^{-21}	Thermo
b	cc^2/(particle^2 sec)			1.7×10^{-33}	24
c	cc/(particle sec)			4.7×10^{-13}	b/K_1
K_2				227	Thermo
d	cc/(particle sec)	1.44×10^{-12}			
e	cc/(particle sec)	6.3×10^{-15}			d/K_2
f	cc/(particle sec)	1.56×10^{-10}			
ig/h	cc^2/(particle^2 sec)	(O_2) 5.0×10^{-32}			
		(Ar) 3.3×10^{-32}			
$K_1(d+f)$	cc^2/(particle^2 sec)	5.7×10^{-31}	4.8×10^{-31}	5.4×10^{-31}	3
j	cc^2/(particle^2 sec)			1.17×10^{-32}	23

elementary rate constant d is evaluated

$$d = 1.44 \times 10^{-12} \text{ cc/(particle sec)} \quad (66)$$

By subtracting d in eq 66 from the sum $d + f$ in eq 63, we obtain the elementary rate constant f.

$$f = 1.56 \times 10^{-10} \text{ cc/(particle sec)} \quad (67)$$

The observed half-life and modulation amplitude of ClO, eq 53 and 54, can be combined in another way to yield a straightforward kinetic expression

$$\sigma_1(2700 \text{ Å})L/2A_1t_1 = e + iK_3[M] = 1.22 \times 10^{-12} \text{ cc/(particle sec)} \quad (68)$$

As will be shown below, for 1 atm total pressure the term e is negligible compared to iK_3. Thus replacing [M] by [O_2] we obtain

$$iK_3 = 5.00 \times 10^{-32} \text{ cc}^2\text{/(particle}^2 \text{ sec)} \quad (69)$$

This term may be regarded as ig/h, the product and ratio of constants involving the intermediate Cl_2O_2, or it may be regarded as k_3, the elementary third-order rate constant for the reaction

$$ClO + ClO + O_2 \xrightarrow{k_3} Cl_2 + 2O_2 \quad (70)$$

Under the conditions of Table I the concentrations of radicals under steady-rate illumination can be calculated

$$[ClO]_s = A_1/\sigma_1 L = 1.06 \times 10^{12} \text{ particles/cc}$$

$$[ClOO]_s = A_2/\sigma_2 L = 0.29 \times 10^{12} \text{ particles/cc} \quad (71)$$

$$[Cl]_s = [ClOO]_s/K_1[O_2] = 3.26 \times 10^{12} \text{ particles/cc}$$

The rate constants and other quantities evaluated from the data are summarized in Table IX.

The study of the effect of inert gas M on the rate of destruction of ClO was done under conditions different from those of Table I. The observation wavelength was in the region of continuum absorption, 2577 Å. Experimental conditions and results are given in Table VI. To correspond to the conditions of Table VI, eq 68 is rewritten

$$L/A_1t_1 = 2e/\sigma_1(2577 \text{ Å}) + 2iK_3[M]/\sigma_1(2577 \text{ Å}) \quad (72)$$

A plot of the data in Table VI on a linear scale, including Clyne and Coxon's point at very low pressures, conforms to relation given by eq 72, that is, a linear plot with finite intercept. However, the data have sufficient scatter that extrapolation to zero pressure to evaluate e/σ is not reliable. On the other hand, the equilibrium constant K_2 is the ratio of rate constants d/e; *cf.* eq 34. Thus the value of e can be estimated from the value of K_2, eq 57, and the value of d, eq 66

$$e = d/K_2 = 6.34 \times 10^{-15} \text{ cc/(particle sec)} \quad (73)$$

The value of iK_3, where M is O_2, was given by eq 69. Thus use of the relation $S = 2(e + iK_3[M])$ and the value of $\sigma_1(2577)$, eq 55, gives the numerical values of S' and S'' for the empirical eq 33. The (heavy) calculated curve in Figure 15 is thus based on e and iK_3 as evaluated under other experimental conditions.

$$L/A_1t_1 = 2.63 \times 10^3 + 2.07 \times 10^{-14}[O_2] \quad (74)$$

Although the calculated curve does not go precisely through the observed points, it does explain many otherwise puzzling features. At about 1 or 2 Torr, Clyne and Coxon were in a region of [M] where the rate constant is largely given by the constant term e, and thus their rate was largely independent of M. Porter and coworkers observed much higher values of the overall rate constant, because the term $iK_3[M]$ was an important part of the whole. Porter found no activation energy and no inert gas effect on this rate constant. Meanwhile, Clyne and Coxon have found the activation energy to be about 2.5 kcal/mole, and we have found an inert gas effect. In Porter's system, flash photolysis gave a large, adiabatic temperature rise. A reduction of total pressure would lead to an increased adiabatic temperature and thus an increased reaction rate, but the M-gas effect would tend to give a lower reaction rate. Thus the near cancellation of these two effects may have caused Porter to miss both of them.

The efficiency of Ar as a chaperon gas for reaction ig/h is distinctly less than that for oxygen as can be seen by Figure 15. Whereas iK_3 for oxygen is 5.0×10^{-32} cc^2/(particle^2 sec), the value for Ar (where M is Ar) is

$$iK_3 = 3.3 \times 10^{-32} \text{ cc}^2\text{/(particle}^2 \text{ sec)} \quad (75)$$

Evaluation of Rate Constants from the Mechanism from Infrared Data. A particular set of reactant concentrations and light intensity, different from that used in the ultraviolet system, was used to obtain the observable lifetime of ClOO, t_2, and its modulation amplitude A_2. The numerical values are given in Table I. These quantities are combined in a way analogous to that used in the ultraviolet study. Since the ClO radical was not observed in the infrared system, the infrared study gives much less kinetic data than the ultraviolet study. The

infrared analogs of eq 61–63 are

$$\frac{K_1(d+f)}{(1+K_1[O])^2} = 4.01 \times 10^{-31}\ \text{cc}^2/(\text{particle}^2\ \text{sec}) \quad (76)$$

$$K_1(d+f) = 4.76 \times 10^{-31}\ \text{cc}^2/(\text{particle}^2\ \text{sec}) \quad (77)$$

$$d+f = 1.31 \times 10^{-10}\ \text{cc}/(\text{particle sec}) \quad (78)$$

As in eq 64 the observed modulation amplitude of ClOO at 1443 cm^{-1} leads to the absolute cross section for absorption of infrared radiation by the ClOO radical

$$\sigma_2(1443\ \text{cm}^{-1}) = 0.78 \times 10^{-19}\ \text{cm}^2 \quad (79)$$

The steady-state concentration of ClOO in the infrared system is

$$[ClOO]_s = 2.67 \times 10^{11}\ \text{particles/cc} \quad (80)$$

The values of these quantities and those found from the ultraviolet data are summarized and compared in Table IX. It is to be noted that there is satisfactory agreement between the rate laws observed and the rate constants evaluated as observed in the infrared and as observed in the ultraviolet system.

Consistency Tests. In simplifying the rate expression as derived from the mechanism, certain assumptions were made. Now that the rate constants in the mechanism have been evaluated from kinetic data, these assumptions can be tested.

A key assumption in the analysis of the mechanism is that chlorine atoms are in equilibrium with ClOO, by way of reactions b and c. The way to test this assumption in to evaluate the steady-state concentrations of Cl, ClO, and ClOO from the mechanism and to use the observed rate constants to calculate the relative rates of reactions b, c, d, e, and f. These calculations will be carried out for the conditions of Table I. The steady-state concentrations of radicals are given by eq 71. The various rates are

$$\begin{aligned} b[Cl]_s[O_2][M] &= 4 \times 10^{18}\ \text{particles/(cc sec)} \\ c[ClOO]_s[M] &= 4 \times 10^{18}\ \text{particles/(cc sec)} \\ d[Cl]_s[ClOO]_s &= 2 \times 10^{12}\ \text{particles/(cc sec)} \\ e[ClO]_s^2 &= 1 \times 10^{10}\ \text{particles/(cc sec)} \\ f[Cl]_s[ClOO]_s &= 2 \times 10^{14}\ \text{particles]/(cc sec)} \\ j[Cl]_s^2[M] &= 4 \times 10^{12}\ \text{particles/(cc sec)} \end{aligned} \quad (81)$$

Each rate (of the forward reaction b and of the reverse reaction c) in the equilibrium K_1 is far greater than that of any other reaction involving either Cl or ClOO. Thus the approximation of assuming Cl and ClOO to be in equilibrium, eq 36, is an excellent one in this system. (It should be noted that under conditions of flash photolysis, this statement is no longer true.)

In simplifying eq 37, we made the assumption given by eq 38. The numerical aspects of this assumption are now seen to be $1.3 \times 10^{10} \ll 1.5 \times 10^{14}$. Thus the transition from eq 37 to eq 39 is fully justified.

Another simplifying assumption is given by eq 45. Although K_3 was not evaluated, it can be estimated to be within an order of magnitude or two of K_1. If it is about equal to K_1 the numerical aspects of the assumption are $10^{-8} \ll 1$. This inequality is so strongly verified that even with maximum uncertainty in K_3, it is still valid to replace eq 44 by eq 46.

Equation 41 was simplified to eq 43 upon the assumption of (82). The numerical values of all of these

$$j[M]/K_1[O_2] \ll (d+f) \quad (82)$$

constants are now known, so this inequality is

$$3.2 \times 10^{-12}[M]/[O_2] \ll 157 \times 10^{-12}$$

When the system consists only of Cl_2 and O_2, with O_2 equal to or greater than Cl_2, this inequality is satisfied. However, when an inert gas is added in great excess over O_2, then the more bulky relation, eq 41, should be used rather than the simplified eq 43. Specifically, it should be noted that the entire expression, $d + f + j[M]/K_1[O_2]$, cancels out of the equations that determine the M dependence of the ClO destruction, and (72) is in no way dependent on the satisfaction of inequality 82.

Another consistency test is to compare our two values of $K_1(d+f)$ with that to be inferred from Porter and Wright's work. The comparisons are given in eq 59, 62, and 76: 5.4×10^{-31}, Porter and Wright; 5.7×10^{-31}, this uv study; 4.8×10^{-31}, this ir study. These three independent determinations of this relatively directly observable quantity are in satisfactory agreement with one another.

To replace the two coupled differential equations (eq 17) by the two separate differential equations (eq 19), it is necessary for the ClOO radical to have virtually zero phase shift. Figure 9 indicates the very limited range of conditions under which this approximation is valid. In general we interpreted data by way of the coupled eq 17, and we used eq 19 only to provide the simple, limiting, physical interpretation of the amplitudes and lifetimes.

Summary

In the gas-phase study of intermediates in the system where Cl_2 is photolyzed in the presence of O_2, we observed an infrared absorption at 1443 cm^{-1}, which is one of the fundamental frequencies identified as ClOO in the matrix-isolation study by Arkell and Schwager.[15] A new spectrum observed in the ultraviolet was shown to be an intermediate with the same kinetic properties as those we observed in the infrared. Thus by combining infrared spectroscopic data with clear-cut kinetic data, we conclude that the new species in the uv is also ClOO.

From the literature and from our study, we are able to express the kinetics of this system in terms of a complex mechanism involving ten elementary reactions and four intermediates, Cl, ClOO, ClO, and Cl_2O_2. By direct observation of two of these intermediates, ClO and ClOO, we were able to derive and confirm a unique set of differential rate equations. From our own studies, from literature values of the absolute cross section for ultraviolet light absorption by ClO and other constants, and from the thermodynamic properties of ClO, we were able to evaluate separate values of seven out of ten elementary rate constants and to evaluate a composite (gi/h) expression for the other three. The cross section for absorption of ultraviolet and infrared radiation by ClOO in the gas phase was also determined. With these rate constants and cross sections, the assumptions made in deriving the rate expressions were verified. The elementary rate constants and other kinetic parameters are summarized in Table IX.

This kinetic (as well as gas-phase spectroscopic) study of ClOO is the first to be reported. The kinetics and

ultraviolet spectrum of ClO have been studied repeatedly. Other investigations have agreed that ClO reverts to Cl_2 and O_2 by a process second order in ClO, but the reported second-order constants have shown large variations between authors. We have confirmed and characterized the foreign gas catalysis of this process, which accounts for much of this discrepancy.

Acknowledgment. This article summarizes the results of two Ph.D. theses, one[19] supported by the Atomic Energy Commission (Inorganic Materials Division of the Lawrence Radiation Laboratory) and the other[18] supported by the National Air Pollution Control Administration, Department of Health, Education, and Welfare, Public Health Service, Grant AP-00104. The original intention was to use the well-known chlorine–oxygen system and the well-characterized ClO intermediate as a calibration for the new molecular modulation method. With the discovery of ClOO and new kinetic features, the intended brief calibration was expanded to this full study. We are deeply grateful to both the AEC and the National Air Pollution Control Administration for long-term support of this work, and to the National Science Foundation for a Traineeship for E. D. M.

Isotope Exchange Rates. VII. The Homogeneous Atom Switching Reaction between Oxygen Molecules

H. F. Carroll and S. H. Bauer

Contribution from the Department of Chemistry, Cornell University, Ithaca, New York 14850. *Received June 26, 1969*

Abstract: The atom switching process, $^{32}O_2 + {}^{36}O_2 = 2{}^{34}O_2$, with the reactants highly diluted in argon, was studied behind reflected shocks in single-pulse shock tubes over the temperature range 1150–1600°K. Oxygen mole fractions varied from 0.0005 to 0.02, and the total density ranged from 1×10^{-2} to 4.5×10^{-2} mole $l.^{-1}$. The $^{36}O_2$ gas was prepared by electrolyzing 97.6 atom % ^{18}O water. Compositions of the reactant and product mixtures were estimated with a CEC No. 21-103 mass spectrometer. The exchange rate data were fitted equally well by two empirical rate expressions: $d[^{16}O^{18}O]/dt = 4 \times 10^{12} \exp[-(41 \pm 4)/RT][^{32}O_2][^{36}O_2]$ moles $l.^{-1}$ sec^{-1}, and $d[^{16}O^{18}O]/dt = 7 \times 10^{10} \exp[-(39 \pm 4)/RT]([^{32}O_2] + [^{36}O_2])^2$ moles $l.^{-1}$ sec^{-1}. The possible effects of impurities (particularly of N_2 and D_2) were tested and shown to be of no consequence. Experimental conditions exclude the possibility that the measured exchange was due to an atomic abstraction mechanism. These rate expressions can be rationalized on the basis of a two-level vibrational excitation model, when slightly different assumptions are introduced. The assumptions are consonant with energy-transfer efficiencies reported for oxygen–oxygen collisions but not with the reported vibrational relaxation times for oxygen–argon collisions. The possible reasons for this disagreement are discussed, and the differences between the oxygen exchange and other homogeneous exchanges are also examined.

Four-center metatheses are used infrequently as elementary steps in kinetic mechanisms, yet they constitute a reaction type which conceptually cannot be ignored. In conventional kinetic investigations, wherein radicals play a dominant role (generated not infrequently by unspecified initiating steps, such as stray irradiation or surface reactions), molecules switch atoms by displacement or by abstractions which have comparatively low activation energies. However, because the four-center homogeneous metathesis is possibly the oldest elementary step postulated by chemical kineticists, it is challenging to discover conditions wherein it dominates the course of a reaction, and to determine the energetic and geometric parameters which control the relative efficiencies for such reactions in molecular encounters.

After half a century, during which many generations of chemists were told that the reaction $H_2 + I_2 \rightarrow 2HI$ was an experimentally demonstrated example of a four-center homogeneous metathesis (perhaps the only one), Sullivan[1] showed that (a) above ≈800°K most of the HI was produced *via* a chain, analogous to the course followed by the other hydrogen–halogen reactions; and (b) at lower temperatures, both the thermal and photochemical data are best interpreted in terms of a two-step process

$$I_2 \rightleftharpoons 2I \qquad \text{(eq)}$$

$$2I + H_2 \longrightarrow 2HI \qquad \text{(rate limiting)}$$

However, almost concurrently the potential of shock tubes for the study of strictly homogeneous high-temperature reactions was recognized[2,3] and exploited for the investigation of several H/D atom exchanges under conditions which indicated, with a high degree of probability, that the products pass through a four-center transition state.[4–9] In two more investigations, using

(1) J. H. Sullivan, *J. Chem. Phys.*, **46**, 73 (1967), and previous publications.

(2) H. S. Glick, J. J. Klein, and W. Squire, *ibid.*, **27**, 850 (1957).
(3) S. H. Bauer, *Science*, **141**, 867 (1963).
(4) S. H. Bauer and E. L. Resler, Jr., *ibid.*, **146**, 1045 (1964).
(5) (a) A. Lifshitz, C. Lifshitz, and S. H. Bauer, *J. Am. Chem. Soc.*, **87**, 143 (1965); (b) A. Burcat and A. Lifschitz, private communication.
(6) (a) S. H. Bauer and E. Ossa, *J. Chem. Phys.*, **45**, 434 (1966); (b) A. Lifshitz and A. Burcat, *ibid.*, **47**, 3079 (1967); (c) D. Lewis, Cornell University, unpublished results.
(7) W. S. Watt, P. Borrell, D. Lewis, and S. H. Bauer, *J. Chem. Phys.*, **45**, 444 (1965).
(8) A. Burcat, A. Lifshitz, D. Lewis, and S. H. Bauer, *ibid.*, **49**, 1449 (1968).
(9) D. Lewis and S. H. Bauer, *J. Am. Chem. Soc.*, **90**, 5390 (1968).